energy&fuels

Article

Cite This: Energy Fuels 2019, 33, 5422−5429

pubs.acs.org/EF

Effects of Alkali Metals on the Formation of Particulate Matter and Adsorption of Floating Beads during Zhundong Coal Combustion

Yufeng Zhang,[†,‡] Jing Zhao,[†,‡] Xiaolin Wei,[*,†,‡] Teng Li,[†,‡] Yu Qiao,[§] and Minghou Xu[§]

[†]State Key Laboratory of High Temperature Gas Dynamics, Institute of Mechanics, Chinese Academy of Sciences, Beijing 100190, People's Republic of China

[‡]School of Engineering and Science, University of Chinese Academy of Sciences, Beijing 100049, People's Republic of China

[§]State Key Laboratory of Coal Combustion, Huazhong University of Science and Technology, Luoyu Road 1037, Wuhan 430074, China

ABSTRACT: Zhundong coal plays an important role in China's energy utilization. However, due to its high content of alkali metals, it produces a large amount of particulate matter during combustion. In this paper, the coal was first washed with deionized water to remove the influence of alkali-metal salts. Then, different kinds of Na salts (1% NaC1, 1% Na_2SO_4, and 1% NaAc) were added to the de-alkali coals. The effect of Na salts on the formation of PM_{10} was studied in a high-temperature drop-tube furnace at 1300 °C. After the addition of the Na salts, the amount of particulate matter emission was significantly increased. When 1% NaCl was added to the de-alkali coal, the amount of PM_1 produced was 3.1 times that of the raw coal, while the amount of $PM_{2.5}$ produced was 3 times that of raw coal. After adding 1% Na_2SO_4, the amounts of PM_1 and $PM_{2.5}$ produced were twice those of the raw coal. In addition, floating beads exhibit a good adsorption effect on particulate matter for the combustion of the coal with different Na salts added. The yield of ultrafine and submicrometer particles was significantly reduced when 3% floating beads were added to the de-alkali coal with Na salts added. The reductions of PM_1 were 47.0% for NaCl, 51.0% for Na_2SO_4, and 29.4% for NaAc. Additionally, the adsorption process of floating beads on ultrafine and submicrometer particles is mainly through the reaction between alkali-metal vapors and SiO_2 and Al_2O_3 in the sorbents.

1. INTRODUCTION

The Zhundong coalfield in Xinjiang Province is China's largest fully fitted coalfield with reserves of 213.6 billion tons.[1,2] Due to its large reserves, the coalfield is expected to be China's main energy supply in the near future.[3,4] However, the coal contains a large quantity of alkali metals.[5−7] Especially, the Na content is high, which leads to the generation of a large amount of particulate matter (PM).[8−10] Studies have shown that $PM_{0.1}$ (aerodynamic diameter less than 0.1 μm) generated by Zhundong coal is 4.7 times that of Hulunbeier lignite and 6.1 times that of Shenhua bituminous coal. The PM_1 (aerodynamic diameter less than 1 μm) production of Zhundong coal is 2.1 times that of Hulunbeier lignite and 3.1 times that of Shenhua bituminous coal.[11−15] Every year, many cities in northern China have smoggy weather for many days, which is mainly caused by PM_{10} from coal combustion.[16,17] PM_{10} contains large quantities of toxic and harmful substances, which cause a serious impact on human health.[18−20] Therefore, it is urgent to study the characteristics of the PM formation of Zhundong coal and the adsorption methods.

Gao et al.[9] conducted a study on the initial formation of ultrafine particles of Zhundong coal in a downward Hencken flat-flame burner. It was found that the formation of ultrafine particles is a process of the multicomponent synthesis of mineral precursors. The competition between the devolatilization and coalescence of particles is the most significant. Xiao et al.[21] studied the effects of sodium and soot on the formation of fine particles during the initial stage of coal combustion. It was found that the oxidation of soot and emission of ultrafine mineral particles are the two main factors that influence the fine particle formation. Niu et al.[22] conducted a kinetic study of the formation of $PM_{0.1}$ during coal combustion and found that the elevated flue gas recirculation ratio is detrimental to PM adsorption.

In addition to the above studies on the formation of particulate matter, there are a large number of studies[23−28] on the adsorption characteristics of particulate matter adsorbents. It was found that SiO_2 and Al_2O_3 have obvious chemisorption on particulate matter. Ruan et al.[23] studied the formation of fine particles produced by lignite, which is rich in alkali and alkaline-earth metals (AAEM) as well as sulfur. It was found that 0.4 μm is the transition point of particulate matter. Additionally, the cofiring of high AAEM sulfur coal and high aluminum silicon coal can significantly reduce $PM_{0.4}$. Chen et al.[24] studied coal combustion in a fluidized bed and found that attapulgite suspension can reduce the emissions of $PM_{2.5}$. Sun et al.[25] studied the effect of kaolin on the emission of $PM_{0.2}$ during pulverized coal combustion and found that the $PM_{0.2}$ capture efficiency of kaolin can be effectively improved by acid and sulfate modification. Si et al.[26] performed combustion experiments on coals with NaCl or NaAc added in O_2/N_2 and O_2/CO_2 atmospheres and found that sodium aluminosilicate plays an important role in particulate matter adsorption. Sodium aluminosilicate promotes $PM_{0.5−2.5}$ to form larger particles. Zhang et al.[27] modified montmorillonite with HCl

Received: March 19, 2019
Revised: May 10, 2019
Published: May 13, 2019

DOI: 10.1021/acs.energyfuels.9b00238
Energy Fuels 2019, 33, 5422−5429

Table 1. Proximate and Ultimate Analysis of Coal

proximate analysis (%)				ultimate analysis (%)					
M_{ad}	A_{ad}	V_{ad}	FC_{ad}	C_{ad}	H_{ad}	O_{ad}	N_{ad}	S_{ad}	Cl_{ad}
14.10	10.08	26.22	49.60	58.36	2.12	13.59	0.41	1.34	0.11

Table 2. Composition of Ash

SiO_2	Al_2O_3	Fe_2O_3	CaO	MgO	TiO_2	SO_3	P_2O_5	K_2O	Na_2O
16.61	5.86	15.33	22.66	3.94	0.44	29.18	0.24	0.58	3.20

and polyhydroxy aluminum solution and found that acid modification leads the Si−O bonds to be more susceptible to cracking at high temperatures. After modification by the polyhydroxy aluminum solution, new Si−O−Al bonds are formed. Both these modifications promote the reaction between montmorillonite and alkali metals.

There are many methods for studying the adsorption of PM, but floating beads (FB) are rarely studied as the adsorbent. Floating beads are hollow microspheres, which can be obtained by flotation from the ash of coal. They are generally used as heat-insulating materials because of their low thermal conductivity and high melting point (more than 1600 °C). It has been found that 61.81% SiO_2 and 33.60% Al_2O_3 are mainly contained in the floating beads, which are higher contents than those of the particulate adsorbents currently used, namely, kaolin (approximately 46% SiO_2 and 38% Al_2O_3), attapulgite suspension (approximately 56% SiO_2 and 9% Al_2O_3), and montmorillonite (approximately 60% SiO_2 and 18% Al_2O_3). Moreover, floating beads are thin-walled hollow structures and have a large internal surface. Therefore, floating beads can be a particulate adsorbent with good chemical and physical adsorption.

Based on the above analysis, floating beads were selected as the particle adsorbent for investigation. In this paper, the coal was first washed with deionized water to remove the influence of alkali-metal salts. Then, different types of Na salts (1% NaC1, 1% Na_2SO_4, and 1% NaAc) were added to the coal with the alkali metals removed. The effect of Na salts on the formation of PM_{10} was studied in a high-temperature drop-tube furnace at 1300 °C. Finally, floating beads were added to the de-alkali coal with alkali-metal salts added to study their adsorption. The samples used in this experiment are raw coal, de-alkali coal (DC), DC + 1% NaCl, DC + 1% Na_2SO_4, DC + 1% NaAc, DC + 1% NaCl + 3% FB, DC + 1% Na_2SO_4 + 3% FB, and DC + 1% NaAc +3% FB. The main analytical techniques used are scanning electron microscopy (SEM) and energy-dispersive spectroscopy (EDS).

2. EXPERIMENTAL SECTION

2.1. Experimental Materials. In this paper, the Wucaiwan Zhundong coal is chosen as the experimental object. The coal is dried, ground, and sieved. The pulverized coal having a particle size of 120−160 μm is selected as the experimental sample. The proximate and ultimate analysis of the coal is shown in Table 1. The composition of coal ash is shown in Table 2, and the ash fusibility of the coal is shown in Table 3. As seen from Table 1, the Wucaiwan coal has a low ash content,[29] while the contents of alkali metals and alkaline-earth metals (Na, K, Ca, and Mg) are high.

2.2. Experimental Procedures. The alkali metal Na in Zhundong coal used in this experiment is mainly water-soluble Na. The main forms are NaCl, Na_2SO_4, and $NaHCO_3$. To remove the effect of the water-soluble Na originally contained in the raw coal, the coal was washed with deionized water at a water-to-coal mass ratio of

Table 3. Fusibility of Ash

deformation temp	softening temp	hemispherical temp	fluid temp
1180 °C	1210 °C	1220 °C	1230 °C

Table 4. Chemical Composition of Floating Beads

SiO_2	Al_2O_3	Na_2O	K_2O	CaO	MgO	Fe_2O_3	SO_3
61.81	33.60	0.62	0.93	0.22	0.86	0.44	0.17

50:1. To ensure that the alkali-metal salts were removed, the coal in the deionized water was continuously stirred for 24 h at 60 °C. The concentrations of anions and cations in the filtrate are shown in Table 5. Combining the data of Tables 1−3, it is found that the residual Na

Table 5. Concentrations of Anions and Cations in the Filtrate

cations (mmol/L)				anions (mmol/L)			
Na^+	K^+	Ca^{2+}	Mg^{2+}	Cl^-	SO_4^{2-}	NO_3^-	HCO_3^-
1.332	0.039	0.885	0.684	0.608	1.625	0.027	0.628

in the coal after washing is 36%. The content of Na is 0.0861% in washed coal. Referring to the result of Qi et al.,[30] it can be considered that the water-soluble Na is removed. After the coal was washed, the influence of the original water-soluble alkali metals can be eliminated. Therefore, the effects of different Na salts on the formation of fine particles can be clearly studied by adding Na salts to the de-alkali coal. The coal was then mixed with additives to prepare samples as shown in Table 6. The additives are FB, NaCl, Na_2SO_4, and NaAc. The size of the FB (for adsorption) used in this experiment is 75−150 μm. Its chemical composition is shown in Table 4.

Table 6. Experimental Samples

fuel	additives			weight (%)
sample 1	raw coal	none	none	100:0:0
sample 2	de-alkali coal	none	none	100:0:0
sample 3	de-alkali coal	NaCl	none	99:1:0
sample 4	de-alkali coal	NaCl	FB	96:1:3
sample 5	de-alkali coal	Na_2SO_4	none	99:1:0
sample 6	de-alkali coal	Na_2SO_4	FB	96:1:3
sample 7	de-alkali coal	NaAc	none	99:1:0
sample 8	de-alkali coal	NaAc	FB	96:1:3

The experimental system is shown in Figure 1. The experiments were carried out in a drop-tube furnace system, which consists of a feed system, an electric heating furnace, a control cabinet, a gas distributor, and a sampling system. The feeder is a disc vibrating micropowder feeder for continuously feeding coal into the furnace at a set rate (0.26 g/min for coal/additive blend samples). The pulverized coal is burned in the corundum reaction tube inside the furnace. The length of the reaction zone is 1440 mm, and the inner diameter is 40 mm. Three thermocouples are placed in the reaction zone for temperature control, located at 240, 720, and 1200 mm

DOI: 10.1021/acs.energyfuels.9b00238
Energy Fuels 2019, 33, 5422−5429

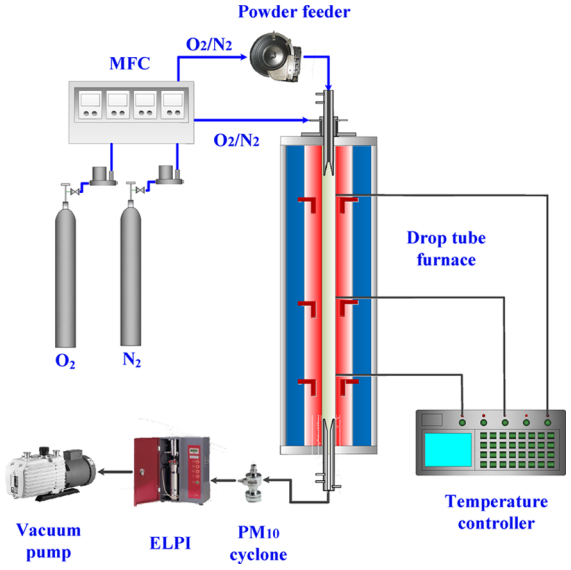

Figure 1. Drop-tube furnace experimental system.

(from top to bottom). The furnace temperature is maintained at 1300 °C. The sampling position is near the position of 1200 mm. For each experiment, 0.78 g of sample was placed in the feeder, which was adjusted to the set rate to maintain the feed time for 3 min. The experimental gas consisted of O_2 and N_2. The rate of O_2 was 2.12 L/min, and the rate of N_2 was 7.9 L/min. The air/fuel ratio in the test was far more than 1. Thus, the furnace temperature was not affected by the fuel combustion.

During the experiment, the particles generated by the coal combustion passed through the cyclone. The particles with a size larger than 10 μm were filtered out.[31] An electrical low-pressure impactor (ELPI) then divided the particles with diameters from 16 nm to 10 μm into 14 stages and collected them on the aluminum foils with Apiezon resin. To prevent the condensation of water vapor, the temperature of the ELPI was always maintained at 140 °C during sampling. The microscopic morphology and composition of the collected particles were obtained by SEM-EDS. It should be emphasized that the particulate matter in this paper refers to fly ash particles with an aerodynamic particle size of less than 10 μm, which are different from the coarse particles in fly ash (particle size greater than 10 μm). These fine particles (PM_{10}) exhibit good fluidity. Their mechanism of generation is also significantly different from that of the coarse particles. Micrometer particles refer to fly ash particles having an aerodynamic particle size of less than 10 μm and greater than 1 μm. Particles having an aerodynamic particle size of less than 1 μm and greater than 0.1 μm are referred to herein as submicrometer particles. Particles having an aerodynamic particle size of less than 0.1 μm are referred to herein as ultrafine particles.

3. RESULTS AND DISCUSSION

3.1. Effects of Na Salts on the Formation of Particulate Matter. Figure 2 shows the distribution of the particulate matter produced by raw coal, de-alkali coal, and the de-alkali coal with Na salts added (DC + 1% NaCl, DC + 1% Na_2SO_4, and DC + 1% NaAc). Dp refers to the aerodynamic diameter of the particulate matter, and m refers to the mass of the particulate matter. log Dp refers to the logarithm of Dp, while dm/dlog Dp refers to the differential of log Dp to m. It can be seen from Figure 2a that the distributions of the particles produced by the samples all show three periods.[32] However, the de-alkali coal samples with Na salts added produce more ultrafine and submicrometer particles than the de-alkali coal. The de-alkali coal with NaCl added produces the largest amount of particulate matter. The emission of PM_1 is 3.8 times that of de-alkali coal, and the emission of $PM_{2.5}$ is 4 times that of de-alkali coal. The amount of PM produced by the de-alkali coal with Na_2SO_4 added is also large. The emission of PM_1 is 2.5 times that of de-alkali coal, and the emission of $PM_{2.5}$ is 2.7 times that of de-alkali coal. The PM_1 produced by the de-alkali coal with NaAc added is 1.38 times that of de-alkali coal, and the emission of $PM_{2.5}$ is 1.4 times that of de-alkali coal. The amounts of $PM_{2.5-10}$ of the five coals do not display significant differences. This indicates that the addition of Na salts mainly increases the emission of ultrafine and submicrometer particles.

Then, SEM was used to analyze the microscopic morphology of the particles deposited on the ELPI impact surface. Figure 3a–c shows the microscopic morphologies of fine particles in three particle sizes (ultrafine, submicrometer, and micrometer particles), which were obtained from four coal samples (DC, DC + 1% NaCl, DC + 1% Na_2SO_4, and DC + 1% NaAc). It can be seen from Figure 3a that the ultrafine particles produced by the de-alkali coal are irregular and do not contain crystals. However, there are crystals that significantly formed in the ultrafine particles of the de-alkali coal with Na salts added, which is also reported in ref 33. Among them, the ultrafine particles of the coal with NaCl added had the highest crystal content, followed by coal with Na_2SO_4 and NaAc added. As shown in Figure 3b, as the size of the particles increases, the quantity of crystals in the submicrometer

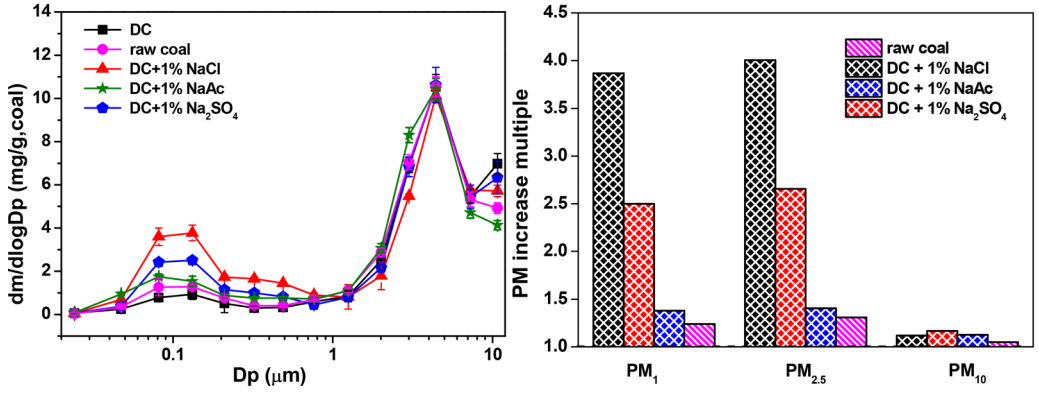

(a) particle size distribution (b) particle concentration increase multiple

Figure 2. Effects of Na salts on the formation of PM with different sizes.

DOI: 10.1021/acs.energyfuels.9b00238
Energy Fuels 2019, 33, 5422−5429

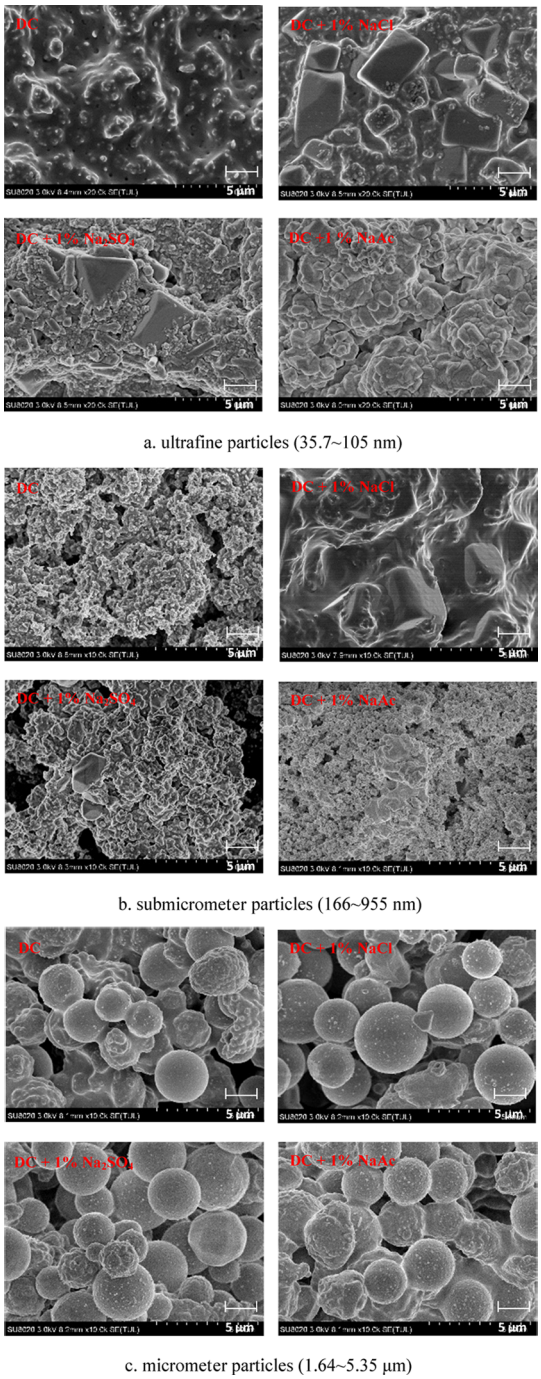

Figure 3. Microscopic morphology of particles.

particles is reduced. In Figure 3c, the micrometer particles mainly show spherical particles, but after careful observation, it is found that the rough surface of the micrometer particles is condensed by gaseous alkali metals as some crystalline matter.

The above phenomenon can adequately explain the particle distribution curves with different Na salts added (Figure 2a). During coal combustion, Na salts volatilize at the high temperature (1300 °C). When the temperature is lowered (240 °C), the gaseous Na salts condense and combine with the coal combustion particulates to form ultrafine and submicrometer particles. Thus, the formation of the crystals will significantly enhance the amount of ultrafine and submicrometer particles. Because the de-alkali coal with NaCl added produces the most crystals, the amounts of ultrafine and submicrometer particles produced by the de-alkali coal with NaCl added are also the highest among the coals with Na salts added. The coal with Na_2SO_4 added and the coal with NaAc added produce less crystalline material, and the amounts of ultrafine and submicrometer particles are also less. For the micrometer particles, although their rough surface contains some crystalline substances, the amount of crystalline substances is small. Thus, the differences in the concentrations of de-alkali coal and de-alkali coal with added Na salts are small.

To illustrate the fine particle formation mechanism of Zhundong coal, the chemical composition of the particles was analyzed by EDS. The numbers 1−4 represent DC, DC + 1% NaCl, DC + 1% Na_2SO_4, and DC + 1% NaAc, respectively. The main elements of ultrafine, submicrometer, and micrometer particles are shown in Figure 4. Compared with the

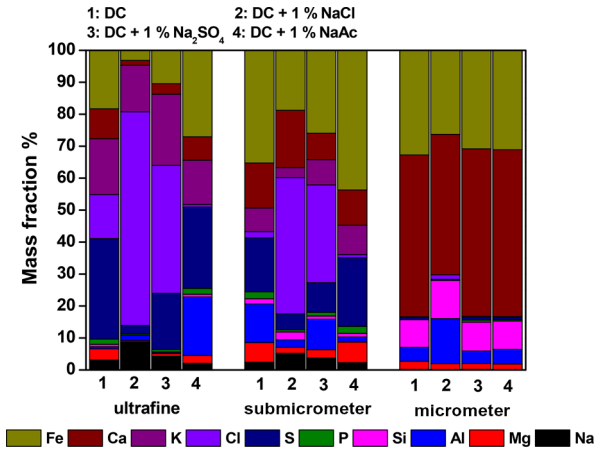

Figure 4. Elemental concentrations of particles of different sizes.

results obtained from SEM, it is indicated that the crystalline substances are mainly chlorine salts of Na, K, Ca, and Fe. The spherical particles in the micrometer particles are mostly aluminosilicates of Na, K, Ca, and Fe. This result is consistent with the results of Li.[14] The composition of the ultrafine particles is mainly Na, K, S, and Cl, and the combined mass of these four accounts for approximately 70% of the ultrafine particles. As the size of the particles increases, the contents of Na, K, S, and Cl in the submicrometer particles decrease, while the relative concentrations of Si, Al, Mg, Ca, and Fe increase, and the micrometer particles mainly contain Fe, Ca, Si, Al, and Mg.

Through the above analysis, it can be found that the formation of PM_1 is a complex physical and chemical process. The PM_1 is mainly formed by two mechanisms.[34,35] The first is the homogeneous nucleation of inorganic vapor. When pulverized coal is burned, some of the inorganic substances (Na, K, Cl, and S) in the coal are easily evaporated at high temperature (1300 °C), which mainly exist in the form of NaOH, Na_2O, KOH, K_2O, HCl, and SO_2. When the gas is released into the flue gas, the temperature is lowered. The NaOH, Na_2O, KOH, and K_2O react with CO_2, SO_2, and HCl to form compounds such as Na_2CO_3, Na_2SO_4, and NaCl, which finally form ultrafine particles by homogeneous nucleation and coagulation. These fine particles ($PM_{0.1}$) mainly contain Na, K, S, and Cl. The second mechanism is that the inorganic vapor condenses unevenly on the surfaces of

DOI: 10.1021/acs.energyfuels.9b00238
Energy Fuels 2019, 33, 5422−5429

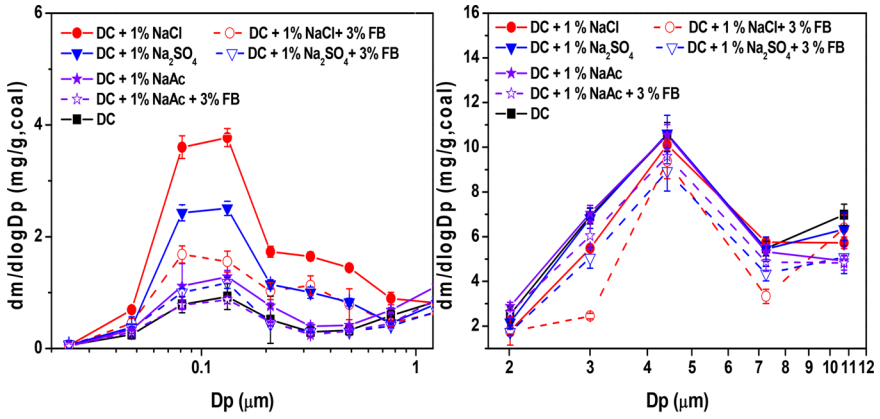

a. ultrafine and submicrometer particles b. micrometer particles

Figure 5. Effect of FB on the particles of coal containing Na salts.

the ash particles of coal fragmentation, which have a large particle size (PM_1). When temperatures are lowered to 240 °C (the flue gas), the growth of the particles is gradually delayed. The particles that collided are sintered together to form submicrometer particles. Therefore, as the size of the particles increases, the contents of Na, K, S, and Cl in the submicrometer particles decrease, while the relative concentrations of Si, Al, Mg, Ca, and Fe increase.

The reason as to why the different sizes of particles have different element contents is related to the gasification ratio of the elements. The temperature at which different elements begin to vaporize is different, and the gasification ratio also varies, which causes their distribution to be different in PM_{10}. The studied elements arranged according to their gasification ratio from large to small are Na > K > Fe > Ca > Si > Al.[35] The most easily vaporized Na and K are first gasified and condense to form particles, which have a small particle size. Therefore, the main elements contained in the ultrafine particles are Na, K, S, and Cl. The gasification ratios of Fe and Ca are intermediate, and thus, their contents in the particulates are substantially equal. SiO_2 and Al_2O_3 are the least gas-vaporizable, and they are rarely present in PM_1 and mainly present in micrometer particles. Thus, the micrometer particles mainly contain Si, Al, Fe, Ca, and Mg, and the micrometer-sized particles contain some Na and K. This is partly due to the fact that there are some alkali-metal crystals on their rough surface and partly due to the reaction of Na and K with SiO_2 and Al_2O_3 to form aluminosilicates.

3.2. Adsorption Characteristics of Floating Beads for the Gas-Phase Alkali Metal. Figure 5 shows the particle distribution of the de-alkali coal with Na salts added and the coal with Na salts and FB added. When pulverized coal with Na salts added combusts, the distribution of the particles exhibits three periods.[32] After the addition of FB, the distribution pattern of the particles is not changed, but the amounts of the first five grades (0.024−0.210 μm) of particles are reduced. Figure 5a shows the particle distributions of ultrafine and submicrometer particles. After FB are added, the amount of ultrafine and submicrometer particle emission is greatly reduced, particularly the coal with NaCl added and the coal with Na_2SO_4 added. The reductions of PM_1 are 47.0% for NaCl, 51.0% for Na_2SO_4, and 29.4% for NaAc. Figure 5b shows the particle size distribution of the micrometer particles. After the addition of FB, the quantity of micrometer particles is also reduced, but the effect is not very obvious. When comparing the amount of particulate matter before and after the addition of FB, it can be seen that FB have a good adsorption effect on particles, and the adsorption effect on ultrafine and submicrometer particles is more obvious. The amount of particles at the first peak of the particle distribution is significantly reduced. For different alkali-metal salts, FB have the best adsorption effect on particles of the de-alkali coal with NaCl added, and the adsorption effect on the particles of the de-alkali coal with Na_2SO_4 is also obvious.

Comparing Figure 6 with Figure 3, it can be observed that the amounts of regular crystals in the ultrafine and submicrometer particles are greatly reduced, and there are essentially no crystalline substances in the particles of the coal with FB and NaAc added. The reason for this phenomenon is mainly due to the adsorption of FB. FB are thin-walled hollow microspheres with large specific surface areas, and their main components are SiO_2 and Al_2O_3. When the coal is burning, Na and K evaporate from the coal, and then, Na and K vapors are

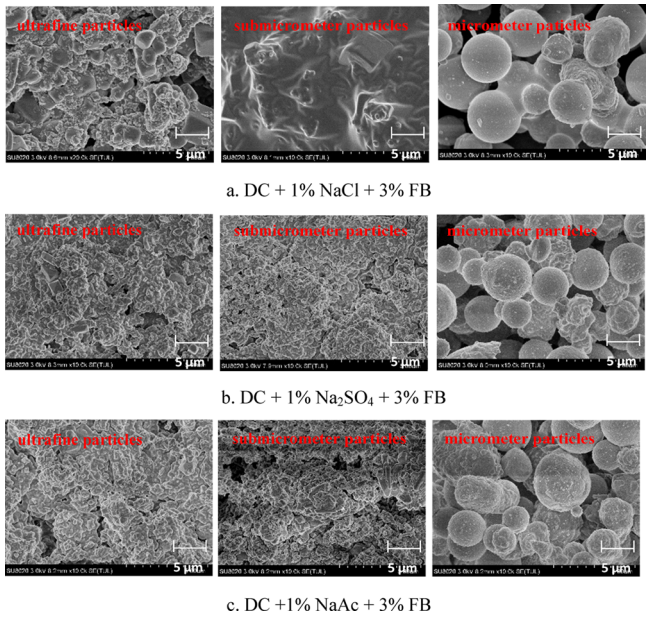

a. DC + 1% NaCl + 3% FB

b. DC + 1% Na_2SO_4 + 3% FB

c. DC +1% NaAc + 3% FB

Figure 6. Microscopic morphology of particles formed by coal with FB added.

DOI: 10.1021/acs.energyfuels.9b00238
Energy Fuels 2019, 33, 5422−5429

adsorbed by tiny pores in the FB during their release. At a temperature of 1300 °C, Na and K react with SiO_2 and Al_2O_3 in FB to form aluminosilicate, which has large particle sizes (more than 10 μm). Therefore, the crystals in ultrafine and submicrometer particles are significantly reduced. The FB also display an adsorption effect on the micrometer particles, but since the micrometer particles are mainly composed of aluminosilicate, they are mainly physically adsorbed. This is consistent with the results of Figure 5.

Figure 4 shows that Na, K, Cl, and S account for a major portion of ultrafine and submicrometer particles. To investigate the effect of FB on the distributions of Na, K, Cl, and S in ultrafine and submicrometer particles, the chemical compositions of the particles of the coal with FB and alkali-metal salts added were analyzed. By comparing Figure 7 with Figure 4, it is found that the contents of Na, K, Cl, and S in the ultrafine and submicrometer particles are reduced, revealing the adsorption effect of FB on the particles. After the addition of the FB, a large number of pores in the FB adsorb Na, K, Cl, and S vapors. At a temperature of 1300 °C, Na and K react with the FB to form aluminosilicate. The physical and chemical adsorption of FB reduces the Na and K vapor contents. After the contents of Na and K vapors are reduced, the nucleation of the alkali-metal vapor decreases. It also leads to a reduced probability of SO_2 and HCl binding to gaseous alkali metals. Thus, some of the SO_2 and HCl are adsorbed by the pores of the FB, and the other part is introduced into the flue gas. The above reasons lead to a decrease in the total amount of the precursor of PM_1. The reduction in particulate precursors weakens two important processes in the formation of ultrafine and submicrometer particles. The two processes are the coagulation of particles colliding with each other and the heterogeneous condensation of inorganic vapor on the surface of the already formed ash particles. Therefore, the amount of final PM_1 production is significantly reduced. The adsorption of FB on ultrafine and submicrometer particles is mainly chemical adsorption, and the chemisorption mechanism of FB for Na and K is shown in reactions 1−4.

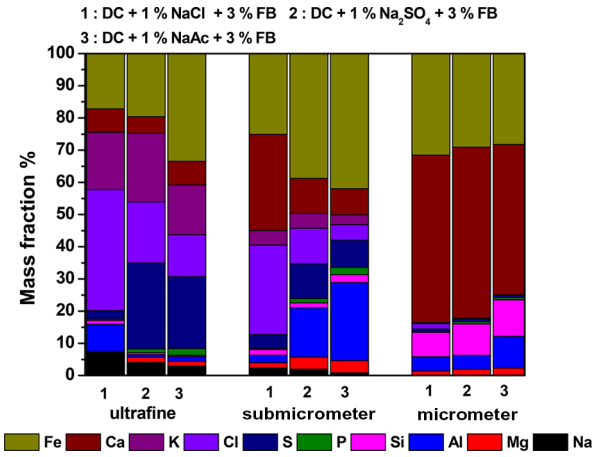

Figure 7. Elemental contents of particulate matter produced by coal with FB added.

$$2MCl(s, g) + SiO_2(s) + H_2O(g) \rightarrow M_2SiO_3(s) + 2HCl(g) \quad (1)$$

$$2MCl(s, g) + Al_2O_3(s) + H_2O(g) \rightarrow 2MAlO_2(s) + 2HCl(g) \quad (2)$$

$$M_2SO_4(s, g) + SiO_2(s) \rightarrow M_2SiO_3(s) + SO_3(g) \quad (3)$$

$$M_2SO_4(s, g) + Al_2O_3(s) \rightarrow 2MAlO_2(s) + SO_3(g) \quad (4)$$

M is Na or K.

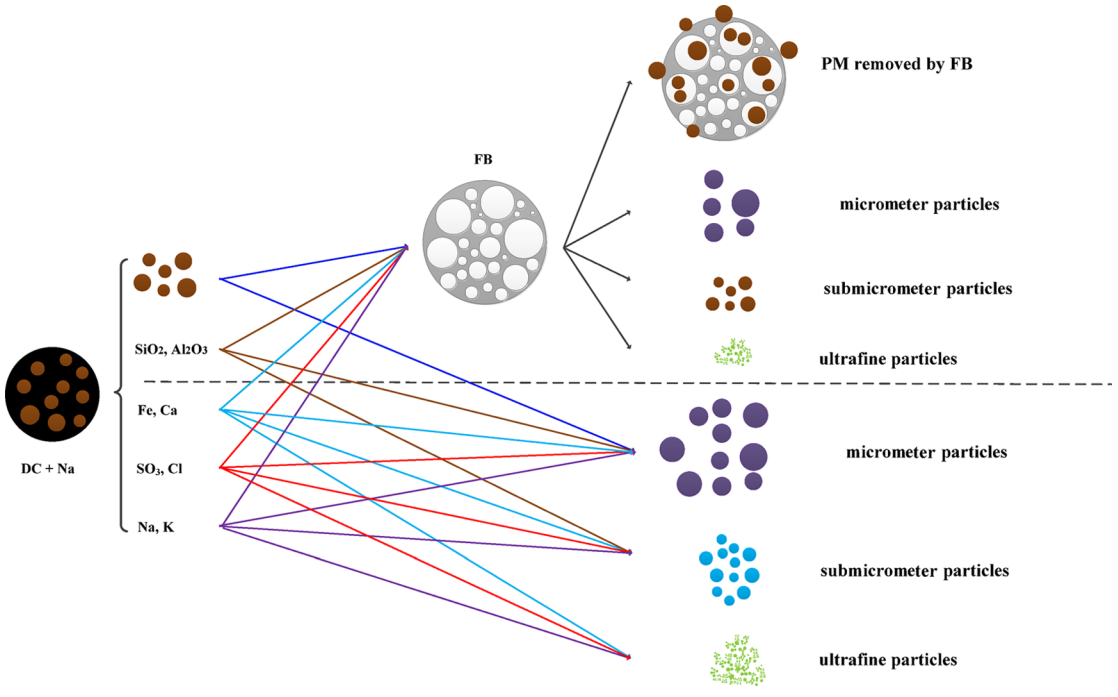

Figure 8. Formation of particles and FB adsorption of particulate matter.

DOI: 10.1021/acs.energyfuels.9b00238
Energy Fuels 2019, 33, 5422−5429

Figure 8 displays the schematic diagram showing the forms of particulate matter from coal and the adsorption of FB of particulate matter. When FB are not added (as shown in the lower half of Figure 8), the inorganic matter in the coal is released during combustion, and the metal elements are first gasified and condense to form particles. When FB are added to the coal (as shown in the upper half of Figure 8), they adsorb the Na and K vapors, which results in a decrease in the coagulation reaction. Thus, the amount of ultrafine and submicrometer particles is correspondingly reduced. Simultaneously, the adsorption of FB also causes the concentrations of other inorganic substances to decrease, and thus, the concentration of PM_{10} decreases overall.

4. CONCLUSIONS

In this paper, the particle formation characteristics of Zhundong coal are studied in a drop-tube furnace at 1300 °C. The experimental samples used are raw coal, DC, DC + 1% NaCl, DC + 1% Na_2SO_4, DC + 1% NaAc, DC + 1% NaCl +3% PB, DC + 1% Na_2SO_4 + 3% FB, and DC + 1% NaAc +3% FB. The effects of Na salts on the formation of particulate matter and the adsorption of floating beads on particulate matter are investigated. The study mainly draws the conclusions described below.

The additions of NaCl, Na_2SO_4, and NaAc have a significant effect on the increase of ultrafine and submicrometer particles. When NaCl is added, the amount of ultrafine and submicrometer particles produced is the most, followed by the coal with Na_2SO_4 added. The main components of ultrafine and submicrometer particles are Na, K, Cl, and S. As the particle size increases, the amounts of Na, K, Cl, and S decrease, while the contents of the elements Ca, Fe, Si, Al, and Mg increase.

The effect of FB on the formation of PM_{10} exhibits different characteristics for different particle sizes. After the addition of FB, they are capable of significantly reducing ultrafine and submicrometer particle emission by adsorbing gaseous alkali-metal inorganic salts. This adsorption is mainly achieved by chemical adsorption. FB also have an adsorption effect on micrometer particles, mainly through physical adsorption. For different Na salts, FB have the most obvious adsorption effect on the particles produced by the coal with NaCl added.

AUTHOR INFORMATION

Corresponding Author

*E-mail: xlwei@imech.ac.cn.

ORCID

Xiaolin Wei: 0000-0002-8856-4032

Notes

The authors declare no competing financial interest.

ACKNOWLEDGMENTS

Financial support for this work was from the National Key R&D Program of China (2016YFB0600601). The authors are also thankful for the suggestions of Wenxia Wang and Jingkun Han on this work.

REFERENCES

(1) Zhou, J.; Zhuang, X.; Alastuey, A.; Querol, X.; Li, J. Geochemistry and mineralogy of coal in the recently explored Zhundong large coal field in the Junggar basin, Xinjiang province, China. *Int. J. Coal Geol.* **2010**, *82*, 51−67.

(2) Wu, X.; Zhang, X.; Yan, K.; Chen, N.; Zhang, J. W.; Xu, X. Y.; Dai, B. Q.; Zhang, J.; Zhang, L. Ash deposition and slagging behavior of Chinese Xinjiang high-alkali coal in 3 MW th pilot-scale combustion test. *Fuel* **2016**, *181*, 1191−202.

(3) Qi, X.; Song, G.; Song, W.; Lu, Q. Influence of sodium-based materials on the slagging characteristics of Zhundong coal. *J. Energy Inst.* **2017**, *90*, 914−922.

(4) Yang, Y.; Lin, X.; Chen, X.; Wang, Y.; Gao, L.; Chen, L. The formation of deposits and their evolutionary characteristics during pressurized gasification of Zhundong coal char. *Fuel* **2018**, *224*, 469−480.

(5) Ding, L.; Gao, Y.; Li, X.; Wang, W.; Xue, Y.; Zhu, X.; Xu, K.; Hu, H.; Luo, G.; Naruse, I.; Yao, H. A novel CO_2-water leaching method for AAEM removal from Zhundong coal. *Fuel* **2019**, *237*, 786−792.

(6) Xu, L.; Liu, H.; Zhao, D.; Cao, Q.; Gao, J.; Wu, S. Transformation mechanism of sodium during pyrolysis of Zhundong coal. *Fuel* **2018**, *233*, 29−36.

(7) Wei, B.; Tan, H.; Wang, X.; Ruan, R.; Hu, Z.; Wang, Y. Investigation on ash deposition characteristics during Zhundong coal combustion. *J. Energy Inst.* **2018**, *91*, 33−42.

(8) Zeng, X.-P.; Yu, D.; Xu, J.-Y.; Wu, J.-Q.; Fan, B.; Xu, M.-H. Study on the effect of adding kaolin to the formation of PM_1 in Zhundong coal combustion. *J. Eng. Thermophys.* **2015**, *36*, 2522−2526.

(9) Gao, Q.; Li, S.; Yuan, Y.; Zhang, Y.; Yao, Q. Ultrafine particulate matter formation in the early stage of pulverized coal combustion of high-sodium lignite. *Fuel* **2015**, *158*, 224−231.

(10) Li, G.; Li, S.; Huang, Q.; Yao, Q. Fine particulate formation and ash deposition during pulverized coal combustion of high-sodium lignite in a down-fired furnace. *Fuel* **2015**, *143*, 430−437.

(11) Li, C.-Z.; Sathe, C.; Kershaw, J. R.; Pang, Y. Fates and roles of alkali and alkaline earth metals during the pyrolysis of a Victorian brown coal. *Fuel* **2000**, *79*, 427−438.

(12) Huang, Q.; Li, S.; Li, G.; Yao, Q. Mechanisms on the size partitioning of sodium in particulate matter from pulverized coal combustion. *Combust. Flame* **2017**, *182*, 313−323.

(13) Wei, X.; Huang, J.; Liu, T.; Fang, Y.; Wang, Y. Transformation of alkali metals during pyrolysis and gasification of a lignite. *Energy Fuels* **2008**, *22*, 1840−1844.

(14) Li, G. D. *Experimental study on formation, evolution and sedimentation characteristics of fine particles in pulverized coal combustion*; Tsinghua University: Beijing, 2014.

(15) Yuan, Y.; Li, S.; Yao, Q. Dynamic behavior of sodium release from pulverized coal combustion by phase-selective laser-induced breakdown spectroscopy. *Proc. Combust. Inst.* **2015**, *35*, 2339−2346.

(16) You, C. F.; Xu, X. C. Coal combustion and its pollution control in China. *Energy* **2010**, *35*, 4467−4472.

(17) Zhang, Z.; Wang, W.; Cheng, M.; Liu, S.; Xu, J.; He, Y.; Meng, F. The contribution of residential coal combustion to $PM_{2.5}$ pollution over China's Beijing-Tianjin-Hebei region in winter. *Atmos. Environ.* **2017**, *159*, 147−161.

(18) Kim, K. H.; Kabir, E.; Kabir, S. A review on the human health impact of airborne particulate matter. *Environ. Int.* **2015**, *74*, 136−143.

(19) León-Mejía, G.; Silva, L. F. O.; Civeira, M. S.; Oliveira, M. L. S.; Machado, M.; Villela, I. V.; Hartmann, A.; Premoli, S.; Corrêa, D. S.; Da Silva, J.; Henriques, J. A. P. Cytotoxicity and genotoxicity induced by coal and coal fly ash particles samples in V79 cells. *Environ. Sci. Pollut. Res.* **2016**, *23*, 24019−24031.

(20) Dmitrienko, M. A.; Legros, J. C.; Strizhak, P. A. Experimental evaluation of main emissions during coal processing waste combustion. *Environ. Pollut.* **2018**, *233*, 299−305.

(21) Xiao, Z.; Tang, Y.; Zhou, J.; Yao, Q. Effect of the interaction between sodium and soot on fine particle formation in the early stage of coal combustion. *Fuel* **2017**, *206*, 546−554.

(22) Niu, Y.; Yan, B.; Liu, S.; Liang, Y.; Dong, N.; Hui, S. Ultra-fine particulate matters (PM_s) formation during air and oxy-coal combustion, Kinetics study. *Appl. Energy* **2018**, *218*, 46−53.

DOI: 10.1021/acs.energyfuels.9b00238
Energy Fuels 2019, 33, 5422−5429

(23) Ruan, R.; Tan, H.; Wang, X.; Li, Y.; Li, S.; Hu, Z.; Wei, B.; Yang, T. Characteristics of fine particulate matter formation during combustion of lignite riched in AAEM (alkali and alkaline earth metals) and sulfur. *Fuel* **2018**, *211*, 206−213.
(24) Chen, H.; Tang, X.; Liang, C.; Wu, X. Attapulgite suspension mitigates fine particulate matter ($PM_{2.5}$) emission from coal combustion in fluidized bed. *J. Environ. Manage.* **2018**, *209*, 245−253.
(25) Sun, W.; Liu, X.; Xu, Y.; Zhang, Y.; Chen, D.; Chen, Z.; Xu, M. Effects of the modified kaolin sorbents on the reduction of ultrafine particulate matter ($PM_{0.2}$) emissions during pulverized coal combustion. *Fuel* **2018**, *215*, 153−160.
(26) Si, J.; Liu, X.; Xu, M.; Sheng, L.; Zhou, Z.; Wang, C.; Zhang, Y.; Seo, Y.-C. Effect of kaolin additive on $PM_{2.5}$ reduction during pulverized coal combustion, Importance of sodium and its occurrence in coal. *Appl. Energy* **2014**, *114*, 434−444.
(27) Zhang, Y.; Liu, X.-W.; Xu, Y.-S.; Sun, W.; Xu, M.-H. Investigation of reducing ultrafine particulate matter formation by adding modified montmorillonite during coal combustion. *Fuel Process. Technol.* **2017**, *158*, 264−271.
(28) Alkan, M.; Hopa, Ç.; Yilmaz, Z.; Güler, H. The effect of alkali concentration and solid/liquid ratio on the hydrothermal synthesis of zeolite NaA from natural kaolinite. *Microporous Mesoporous Mater.* **2005**, *86*, 176−84.
(29) Zhang, X.; Zhang, C.; Yu, S.; Li, X. Effect of coal quality change on CO_2 gasification during quasi-hydrothermal upgrading of Zhundong coal. *J. Fuel Chem.* **2017**, *45*, 1185−1190.
(30) Qi, X. B.; Song, G. L.; Song, W. J. Migration and transformation of alkali metal in the process of quasi-east high alkali coal gasification. *J. Coal* **2016**, *41*, 1011−1017.
(31) Win Lee, S.; Herage, T.; Dureau, R.; Young, B. Measurement of $PM_{2.5}$ and ultra-fine particulate emissions from coal-fired utility boilers. *Fuel* **2013**, *108*, 60−66.
(32) Yu, D.; Xu, M.; Yao, H.; Liu, X.; Zhou, K.; Li, L.; Wen, C. Mechanisms of the central mode particle formation during pulverized coal combustion. *Proc. Combust. Inst.* **2009**, *32*, 2075−2082.
(33) Ruan, R.; Xiao, J.; Du, Y.; Tan, H.; Wang, X.; Yang, F. Effect of Interaction between Sodium and Oxides of Silicon and Aluminum on the Formation of Fine Particulates during Synthetic Char Combustion. *Energy Fuels* **2018**, *32*, 6756−6762.
(34) Zeng, X.; Yu, D.; Yu, G.; Liu, F. Conversion Behavior of Different Forms of Inorganic Elements to Particulate Matter in Quasi-Oriental Coal Combustion. *J. Coal Sci.* **2019**, *44*, 588−595.
(35) Yu, D.; Xu, M.; Yi, F.; Huang, J.; Li, G. Research progress on the formation mechanism of particulate matter in coal combustion process. *Coal Conversion* **2004**, *27*, 7−12.

DOI: 10.1021/acs.energyfuels.9b00238
Energy Fuels 2019, 33, 5422−5429